J Nanostruct 16(1): 198-213, Winter 2026

RESEARCH PAPER

Unraveling the Nano-Challenge: Plackett-Burman Formulation of Etodolac-Loaded, Folic Acid-Conjugated Nanoliposomes for Colon Delivery

Fatimah M.H. Wais*, Sarmad Al-Edresi

Department of pharmaceutics and Industrial pharmacy ,university of Kufa,Iraq

ARTICLE INFO

Article History:
Received 05 August 2025
Accepted 25 October 2025
Published 01 January 2026

Keywords:
Colon cancer
Cytotoxicity
Etodolac
Nanoliposome
Plackett Burman design

ABSTRACT

This study aimed to formulate targeted nanoliposomes for cancer cell delivery. Liposomes were prepared using the thin-film hydration method, with optimization achieved through a Plackett-Burman design of experiments. Folic acid (FA) was employed as a ligand for targeted delivery. The independent variables included DSP weight, cholesterol weight, solvent volume, solubilization temperature, evaporation speed, rehydration temperature, rehydration rotation speed, extrusion number, and freeze-thaw cycles. The dependent variables (responses) were particle size, polydispersity index (PDI), entrapment efficiency (EE), and loading capacity (LC). The particle sizes of all formulations ranged from 99.1 to 250 nm, and the entrapment efficiencies ranged from 56.1% to 88.7%. The optimized formulations were characterized using FESEM, which revealed spherical liposomes without aggregation. DSC and FTIR analyses indicated the drug's transformation to an amorphous state. MTT assays on SW480 cell lines confirmed the formulations' safety. Cytotoxicity assays on SW480 cells demonstrated time- and concentration-dependent cytotoxicity. The IC50 values were: pure etodolac (713.72 ± 4.85 µg/mL at 24 hours, 536.98 ± 6.23 µg/mL at 48 hours), non-targeted liposomes (F1: 602.03 ± 2.8 µg/mL at 24 hours, 419.33 ± 3.55 µg/mL at 48 hours), and targeted liposomes (F2: 554.6 ± 9.12 µg/mL at 24 hours, 128.88 ± 5.26 µg/mL at 48 hours). Cellular etodolac uptake was measured as 12.54 ± 0.078 µg per 10^4 cells for pure etodolac, 20.48 ± 0.19 µg per 10^4 cells for F1, and 26.31 ± 0.11 µg per 10^4 cells for F2. The optimized formulations exhibited good stability over two months.

How to cite this article
Wais F., Al-Edresi S. Unraveling the Nano-Challenge: Plackett-Burman Formulation of Etodolac-Loaded, Folic Acid-Conjugated Nanoliposomes for Colon Delivery. J Nanostruct, 2026; 16(1):198-213. DOI: 10.22052/JNS.2026.01.018

INTRODUCTION

Nanoparticles, generally measuring 1-100 nanometers, possess unique physical and chemical properties due to their tiny size. These properties, such as quick dissolving and extended time in the body, make them attractive for creating new and improved drug delivery systems [1]. We've seen lots of progress in nanotechnology for drug delivery, and lipid-based nanoparticles are a real standout. Things like micelles, solid lipid nanoparticles (SLNs) [2], and nanostructured lipid carriers (NLCs) have proven really effective.

* *Corresponding Author Email: fatimam.al-khahi@uokufa.edu.iq*

Liposomes, a specific type of lipid-based nanoparticle, are especially popular. They're used a lot because they can improve how well drugs dissolve, how precisely they target the right cells, how long they stay in the body, and how effectively they reach their target [3] [4]. The liposomes can be defined as tiny spherical bubbles made of lipids. They have a water-loving inside and a water-fearing outside, which means they can hold drugs inside [5]. Plus, their outer layer can merge with cell membranes, which helps the drug get where it needs to go and prevents it from being eliminated too quickly. That's why they're such a go-to choice for drug delivery. Conventional liposomes are usually made with natural phospholipids and cholesterol [5]. The problem is, these natural phospholipids tend to break down through oxidation and hydrolysis, which makes the liposomes less stable. Even so, phosphatidylcholine (PC), a neutral phospholipid, is the most common ingredient when making liposomes [6].

The main challenge with liposomes is that they tend to get snatched up by cells in the mononuclear phagocyte system (MPS), mostly in the liver and spleen. This means they're cleared from the bloodstream pretty quickly. So, unless you're targeting a disease specifically within the MPS, this rapid clearance really limits how well the drug can reach other parts of the body. Scientists believe that this quick removal happens because serum proteins glom onto the liposomes, a process called opsonization, which then flags them for pickup by the liver and spleen [7].

However, to solve these problems of liposomes by modify their surface. Back in the early 1990, some researchers figured out that adding polyethylene glycol (PEG) to the surface of liposomes makes them more stable and helps them stick around in the body longer. PEG is super water-loving, and when it's attached to the liposome, it creates a stable layer of water around it. This watery shield helps prevent the liposomes from interacting with proteins and cells in the blood, which is important because these interactions can lead to the liposomes being recognized and cleared from the body too quickly [8]. Basically, the PEG coating stops proteins from sticking to the liposomes, which keeps them circulating for longer. So, to precise with drug delivery, you can add a "homing device" to the liposome's surface [9]. This is called targeted delivery, and it basically involves attaching a targeting ligand – think of it like a key – to the liposome so it can unlock and deliver its payload specifically to the right cells [8].

There are many types of these "keys" you can use, like antibodies, bits of DNA or RNA called aptamers, peptides (short chains of amino acids), proteins like transferrin, or even small molecules like vitamins, like folic acid [10]. There are many considerations to choose the right "key," like: how much of the target it's designed to find is actually on the cell you're aiming for, how well the cell takes up the liposome once the "key" fits, and how much of the target molecule the "key" actually covers up [11,12].

Colorectal cancer (CRC) stands as a prevalent and preventable malignancy, ranking as the third most commonly diagnosed cancer among both sexes in the United States [13]. The widespread adoption of colonoscopy has led to increased detection rates, often at early or advanced stages. Globally, CRC constituted a significant health burden, with millions of new cases and hundreds of thousands of fatalities reported in 2018 alone [14]. While incidence and mortality rates have exhibited a declining trend in recent years, CRC remains a substantial public health concern. NSAIDs have been one of the most promising agents in the chemoprevention of colorectal cancer [15]. The main anticancer activity of NSAIDs is thought to be a suppression of prostaglandin E2 synthesis via COX-2 inhibition, which causes a decrease in tumor cell proliferation, angiogenesis, and increases apoptosis [16,17].

Etodolac (ETD), a selective COX-II inhibitor NSAID, is used to treat rheumatoid arthritis (RA) and has shown promise in cancer treatment due to its antiproliferative and antimetastatic effects [18]. ETD's half-life is only around 7 hours; it needs to be taken frequently, typically, at a dose of 200mg twice a day [19,20]. Research also suggests it has anti-tumor properties against various cancer cells. As a selective COX-2 inhibitor (ten times more selective for COX-2 than COX-1) [18,21], etodolac can reduce inflammation without the common gastrointestinal side effects like irritation, ulcers, or bleeding often seen with other NSAIDs. This is because COX-2 inhibitors don't interfere as much with the prostaglandins that protect the stomach lining and regulate kidney blood flow.

The aim of study to formulated target nanoliposome loaded etodolac toward colon cancer cell to improve their target efficacy by

enhance cellular uptake and improve accumulation of drug at site of action and reduce side effect.

MATERIAL AND METHOD

Material

DSPC, DSPE-PEG2000, and 25 mm diameter polycarbonate filters, with pore sizes of 0.1, and 0.2 micrometers were suppliers from Avantis ® Polar lipids, Merck, USA. Etodolac and cholesterol 99%, were purchased from Shanghai Macklin Biochemical Co.Ltd / China. Acetonitrile 99%, methanol 99.8%, chloroform 99.8%, and water 100% are HPLC grade purchased from HiMedia Laboratories Pvt. Ltd. in India. The used vials were purchased from CKlab in China. Phosphate buffer tablet saline from Fischer Scientific, UK.

Method

Preparation and characterization of liposomes loaded etodolac

Optimization of the factors using Plackett Burman design

Optimizing the factors influencing liposome preparation is crucial for establishing a reliable and successful production procedure. The independent variables considered were: DSPC weight (X1), cholesterol weight (X2), solvent volume (X3), solubilization temperature (X4), evaporation speed (X5), rehydration temperature (X6), rehydration rotation speed (X7), extrusion number (X8), and freeze-thaw cycles (X9). The dependent variables (responses) were particle size (Y1), polydispersity index (PDI, Y2), entrapment efficiency (EE, Y3), and loading capacity (LC, Y4), as detailed in Table 1. An 11-run Plackett-Burman design was employed using Design-Expert software version 13, which facilitated the generation of figures and ANOVA analysis. Based on preliminary studies, appropriate low and high levels for each factor were selected [6]. To assess the normality of the unselected factors' distribution, the Shapiro-Wilk test was conducted. A p-value greater than 0.1 was required to consider the factors as having a significant effect and to justify their inclusion in the model

Preparation of liposome using thin film hydration method

Liposomes were prepared using the thin-film hydration method [4]. According to the experimental design, DSPC (10 or 20 mg), cholesterol (5 or 10 mg), and etodolac (8 mg/mL) were mixed and dissolved in 2 or 4 mL of a methanol-chloroform solvent mixture within a 1000 mL round-bottom flask. The resulting clear solution was then subjected to rotary evaporation (Heidolph Instruments GmbH & Co. KG, Germany). The rotary evaporator was set to a temperature of 60 or 65 °C and a rotation speed of 75 or 100 rpm. The solvent was allowed to evaporate, leaving a thin lipid film. This film was further dried under vacuum for 15 minutes to ensure complete solvent removal. Subsequently, the thin film was hydrated with 10 mL of phosphate buffer (pH 7.4) and returned to the rotary evaporator for 10-15 minutes at 65 °C and 100 rpm. The resulting liposomal suspension was visually inspected to confirm complete detachment of the lipid film from

Table 1. Dependent and independent parameters for the Plackett Burman design.

Independent parameters	Level			Dependent parameters
	low	center	high	
Weight of DSPC mg	10	15	20	Particles size
Weight of CHO mg	5	7.5	10	PDI
Solvent volume ml	2	3	4	Encapsulation efficiency
Solubilizing temperature °C	60	63	65	Loading capacity
Evaporation speed rpm	75	88	100	
Rehydration temperature °C	60	63	65	
Rehydration rotation speed rpm	75	88	100	
Extrusion number cycle	5	8	10	
Freezing/Thawing cycle	3	4	5	

the flask walls. The formed suspension, containing multilamellar vesicles, underwent 3 or 5 freeze-thaw cycles, followed by extrusion through a 0.2 µm polycarbonate membrane (Avanti Polar Lipids Inc.), repeated 5 or 10 times. The polycarbonate filter was pre-soaked in phosphate buffer before use in the extruder. The extrusion process was then repeated using a 0.1 µm polycarbonate membrane. The final liposome suspension was clear and transparent in appearance.

Physiochemical characterization of liposome

Particle size PZ, polydisperse index PDI and Zeta potential Evaluation

Particle size (PZ) and polydispersity index (PDI) were determined using correlation photon correlation spectroscopy (PCS) via a nanosizer (ABT-9000 NANO, Laser particle size analyzer) at 25°C and a 90° scattering angle [22]. For each measurement, 3 mL of undiluted liposome suspension was placed into the instrument's glass cell, and each sample was analyzed in triplicate. Zeta potential measurements were similarly performed using a ZetaSizer (Malvern Ltd., Worcestershire, UK) at 25°C, with 3 mL of undiluted liposome suspension per measurement, also conducted in triplicate.

Determination of drug entrapment efficiency (EE) and loading capacity (LC)

Entrapment efficiency (EE) refers to the amount of drug encapsulated within the liposomes, expressed as a percentage of the total drug used in the formulation. [1] Loading capacity (LC) represents the amount of drug encapsulated relative to the total lipid content of the formulation [13]. To determine EE and LC, 5 mL of the drug-loaded liposomal formulation was transferred to an Amicon Ultra-15 mL centrifugal filter tube (MWCO 10 kDa, Sigma-Aldrich International GmbH, Germany) and centrifuged at 5000 rpm for 30 minutes at 4 °C. Following centrifugation, the supernatant in the lower chamber was removed. The upper chamber, containing the drug-encapsulated liposomes, was then washed three times with deionized water, repeating the centrifugation process with the same parameters [15,16,12]. Subsequently, 1 mL of the resulting liposomal suspension was diluted to 10 mL with methanol and analyzed by HPLC (Knauer AZURA). Chromatographic separation was performed using a C18 column, with a mobile phase consisting of methanol, acetonitrile, and water in a ratio of 60:30:10, delivered at a flow rate of 1 mL/min. Detection was carried out at a wavelength of 225 nm. EE and LC were calculated using the following equations:

$$\%\mathrm{EE} = \frac{\text{encapsulated drug}}{\text{total drug}} * 100$$

$$\%\mathrm{LC} = \frac{\text{encapsulated drug}}{\text{total formula of liposome}} * 100$$

Characterization of optimized formula of liposome loaded Etodolac

Morphology of liposome loaded etodolac

Field Emission Scanning Electron Microscopy (FESEM) was employed to determine the surface morphology of the optimized etodolac-loaded liposomes. Imaging was performed using an InspectTM F50 FEI electron microscope. A few drops of the liposomal suspension were deposited onto a carbon-coated copper grid and allowed to dry at room temperature. The samples were then observed at various magnifications at 25°C without staining [16,17].

Differential Scanning Calorimetry DSC

The thermal behavior and melting point of the drug were determined using differential scanning calorimetry (DSC) [23]. DSC analysis was performed for etodolac, DSPC, cholesterol, and etodolac-loaded liposomes using a DSC 60 instrument (Shimadzu, Japan). Prior to analysis, the liposome samples were lyophilized. This involved freezing the samples at -55 °C for one hour, followed by drying in a freeze dryer (Labconco, USA) at -20 °C and 0.01 bar for 24 hours. The lyophilized powder was stored in vials at -20 °C until use. For each sample, 5 mg was accurately weighed and placed in an aluminum pan, which was then sealed with an aluminum lid using a crimper. The samples were heated from 0 to 300 °C at a rate of 10 °C/min. An empty aluminum crucible with a lid was used as a reference. [12,18].

Fourier transform infrared spectroscopy FTIR

Fourier-transform infrared spectroscopy (FTIR) was employed to determine any potential

interactions between the drug and the excipients used in the liposomal formulation [4], [24]. FTIR spectra were acquired for pure etodolac, DSPC, cholesterol, and etodolac-loaded liposomes using an FTIR spectrometer (Shimadzu, Japan). [1] Each sample was individually mixed with infrared-grade potassium bromide (KBr) and subsequently compressed into pellets using a hydraulic press. These pellets were then analyzed within the wavenumber range of 4000 to 400 cm^{-1} [11,22].

In vitro drug release

Etodolac release from the liposomes was measured using a modified dialysis membrane diffusion method [25]. Samples of 2 mL, including pure etodolac and etodolac-loaded liposomes, were placed into dialysis bags with a molecular weight cut-off of 12,000-14,000 Da. The dialysis membranes were soaked overnight in the dissolution media prior to use. Subsequently, the dialysis bags were immersed in 250 mL of either phosphate-buffered saline (PBS) at pH 7.4 and 37°C, or acetate buffer at pH 5.5 and 39°C, maintained at 100 rpm. These conditions simulated plasma and the colon cancer microenvironment, respectively. At predetermined time intervals, 3 mL aliquots were withdrawn and replaced with fresh media to maintain a constant volume. The amount of etodolac released was quantified by HPLC, and the cumulative percentage of drug release was recorded [12].

Kinetic release analyses

Data obtained from in vitro drug release studies of pure etodolac and etodolac-loaded liposomes were utilized to investigate the release kinetics of the formulations. Mathematical models, including zero-order (cumulative percentage of drug release versus time), first-order (logarithm of the cumulative percentage of drug release versus time), Korsmeyer-Peppas (logarithm of the cumulative percentage of drug release versus logarithm of time), and Higuchi (cumulative percentage of drug release versus the square root of time), were applied to determine the dissolution model and elucidate the drug release mechanism from the nanocarrier core [26,27,28,19]. The DDsolver software program, a Microsoft Excel add-in designed for the simulation and comparison of drug dissolution profiles, facilitated the application of these models [12].

Cytotoxicity

The cytotoxicity of various liposomal formulations on SW480 colon cancer cells was evaluated using an MTT colorimetric assay [29,30,31]. SW480 cells, in their logarithmic growth phase, were seeded into 96-well plates and incubated for 24 hours. Subsequently, cells were treated with different concentrations (31.25–1000 µg/mL) of pure etodolac (ETO), blank liposomes (without ETO), and optimized ETO-loaded liposomal formulations for 24 and 48 hours at 37°C. Following these incubations, MTT solution was added, and after a 4-hour incubation at 37°C, the resulting formazan crystals were dissolved in 100 µL of DMSO. Absorbance was measured at 570 nm using a microplate reader (Synergy, FL, USA). Cell viability was then calculated using the following equation:

$$\text{Cell viability}\% = \frac{\text{ODexp} - \text{ODblank}}{\text{ODcontrol} - \text{ODblank}} * 100$$

The OD blank represents the optical density of wells containing only cell culture medium. The OD experiment represents the optical density of wells containing the experimental formulation. OD control represents the optical density of wells containing control cells.

Invitro cellular uptake of etodolac

For the cellular drug uptake study, SW480 cells, a colon cancer cell line obtained from the European Collection of Cell Cultures, were utilized. These cells were cultured in T-flasks using McCoy's 5a medium supplemented with 10% fetal bovine serum (FBS) and maintained in a controlled environment at 37°C, 95% humidity, and 5% CO2. The culture medium was replenished twice weekly, and cells were harvested weekly using TrypLE Express.

Cellular uptake

To quantify cellular drug uptake, SW480 cells were seeded in a 12-well plate at a density of 10,000 cells per well and incubated for 24 hours. Subsequently, cells were treated with either pure etodolac (ETO) or the optimized ETO-loaded liposomal formulation, ensuring each well received an equivalent of 500 µg of ETO. The

plates were incubated at 37°C for the designated period. Following incubation, cells were washed three times with ice-cold phosphate-buffered saline (PBS) to remove any unbound drug. The cells were lysed with a 0.5% Triton X-100 solution in PBS [29,30,31], and the resulting mixture was vortexed for 3 minutes. Cellular debris was then removed by centrifugation. The concentration of intracellular ETO in the supernatant (cell lysate) was determined using high-performance liquid chromatography (HPLC) at a wavelength of 225 nm.

Stability of prepared liposome

To evaluate potential physical or chemical changes, the etodolac (ETO)-loaded liposomes underwent a stability study. The optimized formulations were stored under two conditions: room temperature (25°C ± 2°C) and refrigerated (4°C ± 2°C), both with a relative humidity of 60% ± 5%, for 60 days. The study examined the effect of storage temperature on particle size (PZ), polydispersity index (PDI), and entrapment efficiency (%EE). Samples were withdrawn from each formulation every two weeks, and PZ, PDI, and %EE were measured [19].

RESULTS AND DISCUSSION

Etodolac loaded liposomes for optimization the liposome composition

The thin-film hydration method was successfully employed to prepare a series of etodolac (ETO)-loaded liposomal formulations. To optimize the composition of these liposomes, a design of experiments was utilized, varying independent factors such as DSPC weight (X1), cholesterol weight (X2), solvent volume (X3), solubilization temperature (X4), evaporation speed (X5), rehydration temperature (X6), rehydration rotation speed (X7), extrusion number (X8), and freeze-thaw cycles (X9). The dependent responses measured were particle size (Y1), polydispersity index (Y2), entrapment efficiency (Y3), and loading capacity (Y4).

Optimization the factors for preparation of liposome by using Plackett Burman Design

Screening designs are employed to identify crucial factors during method optimization. These designs enable the evaluation of a substantial number of factors with a comparatively small and manageable set of experiments [2,25,30]. In this study, a Plackett-Burman design of experiments was utilized to optimize nine factors potentially influencing liposome preparation. The results obtained are presented in Table 2. Pareto charts were generated to visualize the significant factors affecting liposome preparation and to optimize the liposome composition. The t-value line on each chart served as a reference threshold; any factor exceeding this line indicated a statistically significant effect ($p \leq 0.05$). All figures were generated using Design-Expert® software.

Statistical analysis revealed that DSPC and evaporation speed (ES) significantly influenced particle size (PZ) ($P \leq 0.05$), as illustrated in Fig. 1A. Solvent volume (SV) significantly affected both loading capacity (LC) and entrapment efficiency (EE) ($P \leq 0.05$), as shown in Figs. 1B and 1C,

Table 2. Composition of Etodolac-Loaded Liposomes and Their Characterization Measurements.

	Independent parameters									Dependent parameters			
Run	X1	X2	X3	X4	X5	X6	X7	X8.	X9	PZ nm Y1	PDI Y2	%EE Y3	%LC Y4
L1	-1	-1	+1	-1	+1	+1	-1	+1	-1	125	0.01	63.7	53.6
L2	+1	+1	-1	-1	-1	+1	-1	+1	+1	199	0.018	65.1	47.3
L3	-1	-1	-1	-1	-1	-1	-1	-1	-1	223	0.011	82.7	69.6
L4	-1	-1	+1	+1	-1	+1	+1	+1	+1	250	0.012	65.3	55
L5	+1	-1	+1	+1	+1	-1	-1	-1	+1	99.1	0.012	64.2	48.9
L6	+1	-1	-1	+1	-1	+1	+1	-1	-1	99.6	0.13	86.2	65.7
L7	-1	+1	+1	-1	-1	-1	+1	-1	+1	177	0.023	56.1	44.9
L8	+1	-1	-1	-1	+1	-1	+1	+1	+1	111	0.027	83.1	63.3
L9	-1	+1	-1	+1	+1	+1	-1	-1	+1	125	0.138	66.6	53.3
L10	+1	+1	+1	+1	-1	-1	-1	+1	-1	111	0.125	57.9	42.1
L11	-1	+1	-1	+1	+1	-1	+1	+1	-1	177	0.01	88.7	71
L12	+1	+1	+1	-1	+1	+1	+1	-1	-1	99.3	0.075	87.5	63.6

respectively. However, none of the selected factors significantly impacted the polydispersity index (PDI) ($P > 0.05$), as depicted in Fig. 1D. In these charts, the t-value line represents the reference for statistical significance; factors exceeding this line indicate a significant effect ($P \leq 0.05$). All figures were generated using Design-Expert® software, as presented in Fig. 1.

The formulations all exhibited nanosized particles, with particle sizes (PZ) ranging from 99.1 to 250 nm and polydispersity indices (PDI) ranging from 0.011 to 0.138. The low PDI values indicate a homogeneous nanoparticle distribution [30,31]. PDI is a critical parameter for assessing storage stability. A narrow size distribution minimizes nanoparticle aggregation, and particles with such a distribution are less susceptible to Ostwald ripening, a process where smaller particles dissolve and larger particles grow, leading to changes in size distribution over time [32].

Predicting the main effects of independent variables on dependent variables is crucial for liposomal development [33], a goal achieved in this study using the Plackett-Burman design. This approach aligns with the findings of Hassan et al. (2015), who demonstrated the design's reliability in optimizing rhamnolipid production from biodegrading bacterial isolates [34]. Employing the Plackett-Burman design significantly reduced the number of experimental trials, consistent with Harshal Ashok et al. (2016), who highlighted its efficacy as a screening method for identifying key independent factors and their influence on dependent variables with minimal runs [35,36].

The study revealed that particle size (PZ) was significantly influenced by both DSPC concentration and evaporation speed (ES). This can be attributed to the increased lipid amount (10-20 mg), which enhances lipid molecule coverage, leading to greater membrane fluidity and larger liposome sizes. Furthermore, higher lipid concentrations can increase membrane rigidity, hindering size reduction during extrusion and resulting in larger vesicles. These findings corroborate those of Anil Kumar et al. (2017), who reported a significant impact of lipid concentration on gedunin-loaded

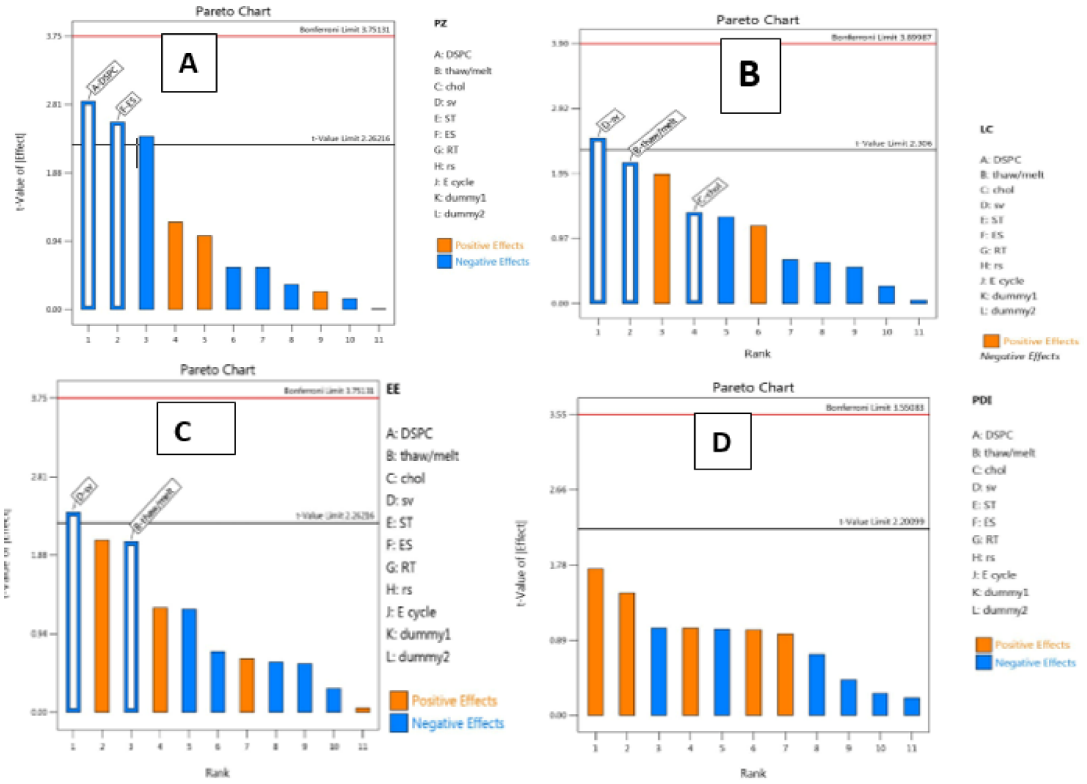

Fig. 1. Pareto chart ranking the standardized effect of selected factors: A: Effect of DSPC on PZ, B: Effect of SV on %LC, C: Effect of SV on %EE, D: Effect of factors on PDI.

liposome size [33] and Somayeh et al. (2018), who also observed a significant effect of phospholipid amount on PZ [37].

Cholesterol concentration also significantly affected PZ (negatively). Increased cholesterol content enhances the hydrophobicity of the bilayer membrane, leading to larger vesicle radii for greater thermodynamic stability. The resulting rigid bilayer structure resists size reduction during sonication, producing larger vesicles [38], a result consistent with the findings of Gyati Shilakari et al. (2016) [39]

The polydispersity index (PDI) was not significantly affected by any of the tested factors, which contradicts the findings of Mahdi Bahrami et al. (2023), who reported a significant influence of phospholipid concentration and hydration time on liposome PDI [12].

Entrapment efficiency (%EE) was significantly affected ($p < 0.05$) by solvent volume (SV) but not by other factors such as DSPC concentration. The %EE ranged from 56.1% to 88.7%, and the loading capacity (%LC) ranged from 42.1% to 71%. These results align with Navneet et al. (2016), who observed that an increased organic solvent volume, leading to higher system viscosity, significantly impacts %EE [40].

Optimization the ETO loaded liposome composition by using Plackett Burman Design

Optimized formulations, chosen for their small particle size, low polydispersity index (PDI), high entrapment efficiency (%EE), and high loading capacity (%LC), were prepared using the previously described thin-film hydration method. The optimal composition for the conventional etodolac (ETO)-loaded liposomes (F1) was a lipid mixture of DSPC and cholesterol (CHO) at a ratio of 12.7:5 (mg), as determined by the Plackett-Burman design. The targeted liposomes (F2) included a lipid mixture of DSPC, CHO, DSPE-PEG2000, and DSPE-PEG2000-FA at a ratio of 12.7:5:1:0.1 (mg). Both formulations (F1 and F2) were then subjected to further characterization, including particle size (PZ), PDI, EE, differential scanning calorimetry (DSC), Fourier-transform infrared spectroscopy (FTIR), in vitro release, and cellular uptake studies.

Physiochemical characterization of optimize liposome

Particle size and size distribution are critical characteristics of liposomes, significantly influencing their suitability for inhalation and parenteral administration [4]. These factors also determine the circulation half-life, biodistribution, and targetability of liposomes, with smaller liposomes exhibiting prolonged circulation compared to larger ones. For drug delivery applications, an average liposome size ranging from 50 to 200 nm is generally considered optimal. The optimized formulations, F1 and F2, demonstrated the following characteristics: F1 (particle size: 111.7 ± 0.11 nm, polydispersity index (PDI): 0.001, entrapment efficiency (%EE): 89.7 ± 0.002%) and F2 (particle size: 125.5 ± 0.01 nm, PDI: 0.027, %EE: 88.6 ± 0.017%)

Furthermore, zeta potential is another essential parameter, reflecting the stability of colloidal systems such as liposomal nanocarriers in suspension [5,41]. It represents the overall net charge on the particle surface, governing the electrostatic interactions between particles. The zeta potential values were -3.20 mV, -10.2 mV, and -13.6 mV for pure etodolac, F1, and F2, respectively.

Surface Morphology Analysis using Field Emission Scanning Electron Microscopy (FESEM)

The surface morphology of the liposomes for formulations F1 and F2 was examined using Field Emission Scanning Electron Microscopy (FESEM). The FESEM images obtained for both formulations revealed spherical nanoparticles with no evidence of aggregation, as depicted in Fig. 2A and B, respectively. The optimized F1 and F2 nanoparticles exhibited sizes of 111.7 ± 0.11 nm and 125.5 ± 1.99 nm, respectively. These FESEM measurements corroborate the particle size analysis obtained through dynamic light scattering.

FTIR

Fourier-transform infrared (FTIR) spectroscopy was employed to determine the chemical composition of the materials used in the etodolac (ETO) liposome formulations. FTIR spectra were obtained for pure ETO, DSPC, cholesterol (CHO), formulation F1, and formulation F2, as depicted in Fig. 2. The characteristic peaks observed in the pure ETO spectrum were also present in the liposomal formulations F1 and F2. These included a strong peak at 1413.82 cm^{-1} (C-H bending), a strong peak at 1741.72 cm^{-1} (carbonyl C=O vibration), a strong peak at 3346.5 cm^{-1} (N-H stretching vibration), a C-H ring vibration peak at 3053.32 cm^{-1}, and

aromatic C-C stretching vibration bands at 1622.13, 1467.5, 1413.82, and 1365.60 cm^{-1}, along with a C-N stretch peak at 1031.92 cm^{-1} (Fig. 2C). [42,43]. These characteristic ETO peaks were consistently observed in the liposomal formulations F1 and F2 without significant deviation (Fig. 2C). The absence of new peaks and the retention of existing peaks in the spectra confirmed the physical and chemical compatibility between the excipients and etodolac, facilitating the development of stable formulations [44].

Notably, the intensity of the ETO characteristic absorption bands was reduced in the liposomal formulations. The N-H stretch of ETO, in particular, showed decreased intensity. This observed change in the ETO peaks, particularly the decreased intensity of the N-H stretch, suggests a structural transformation such as amorphization or complexation, as documented in previous studies [45]. In the context of this study, this reduction in intensity is consistent with the efficient encapsulation of etodolac within the phospholipid bilayers.

The FTIR spectrum of the targeted formulation F2 exhibited additional peaks at 2854.6 cm^{-1} and 2924.09 cm^{-1}, corresponding to the C-H stretching band, which indicates the aliphatic nature of PEG, FA, and DSPE [37], as depicted in Fig. 2C. The infrared spectrum of DSPC showed characteristic vibrational modes consistent with its molecular structure. Notably, strong signals were observed at 1090 cm^{-1}, attributable to the symmetric stretching of the phosphate (PO_2^-) moiety. Further analysis of the spectrum revealed bands indicative of CH_2 bending (1469.7 cm^{-1}), carbonyl (C=O) stretching (1734.01 cm^{-1}), hydroxyl (OH) bending (1640 cm^{-1}), and CH_2 stretching within the acyl chains (2850.76 and 2920.23 cm^{-1}), as illustrated in Fig. 2C. These spectral assignments are consistent with established literature values for DSPC [46].

DSC

Differential scanning calorimetry (DSC) was performed to investigate the crystalline transformation of the optimal formulations [5]. DSC thermograms were obtained for pure etodolac (ETO), cholesterol, DSPC, and liposomal formulations F1 and F2, as depicted in Fig. 2D.

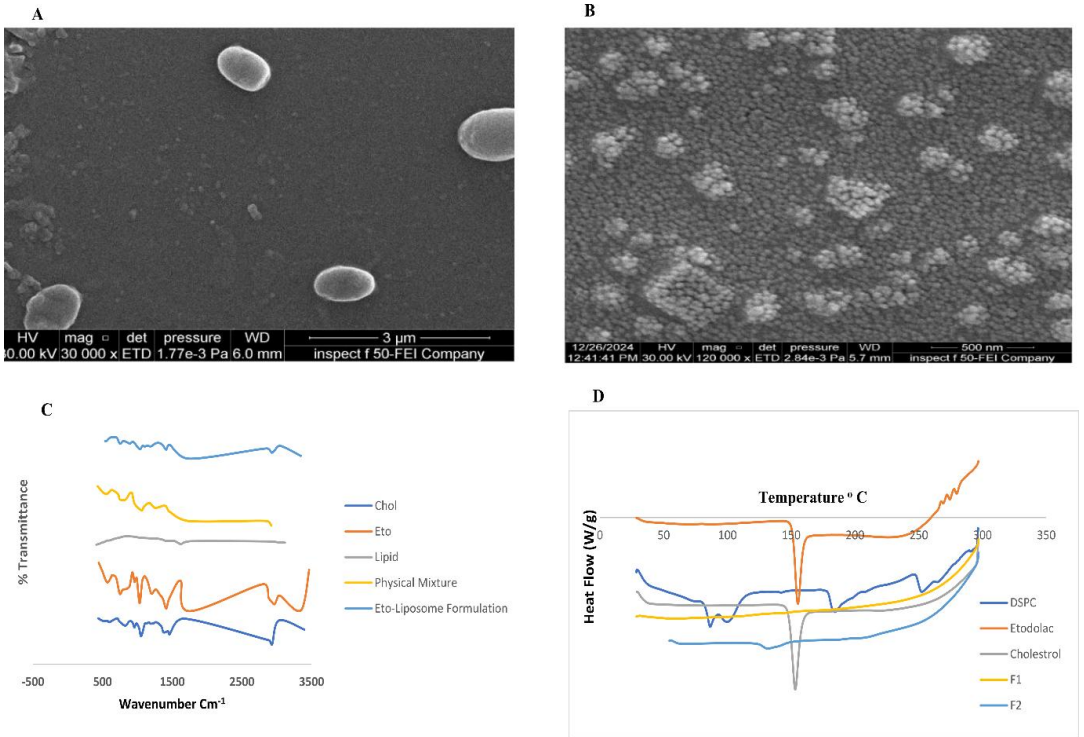

Fig. 2. FESEM images illustrating the morphology of etodolac (ETO)-loaded liposomes for: A: Formulation F1, B: Formulation F2. C: FTIR spectrum of ETO, DSPC, cholesterol, F1, and F2. D: Differential Scanning Calorimetry (DSC) thermograms of etodolac (ETO), DSPC, cholesterol, and Formulations F1 and F2.

Pure ETO exhibited a sharp endothermic peak at 155 °C, indicative of its crystalline nature [47,48]. The DSC thermogram of DSPC showed two prominent endothermic transitions at 127 °C and 182 °C, along with two minor transitions in the 85-100 °C range (Fig. 2D). These multiple endothermic transitions are consistent with prior research, which has documented the complex thermal behavior of phospholipids upon heating, rather than a simple solid-to-liquid transition. As highlighted by Taylor and Morris (1995), water content significantly influences phospholipid structure, leading to the formation of mesophasic or liquid-crystalline states. Cholesterol showed a sharp endothermic transition at 150 °C.

For the ETO-loaded liposomes (F1), no distinct peak was observed (Fig. 3C). This absence of discernible phospholipid transitions suggests the incorporated drug's amorphous state. The observed shift and broadening of the phospholipid transition within the nanoparticles indicate strong interactions among the liposomal components. This observation aligns with previous findings, such as those reported by Abeer Alesknd rany and Ipek Sahin (2020), who demonstrated a significant decrease in the transition temperature of DPPC lipid in liposomes upon interaction with levothyroxine [49].

In ETO-loaded liposomes F1 and F2, broad endothermic peaks were observed at 126 °C and 131 °C, respectively, potentially reflecting the altered thermal behavior of DSPC due to interactions with other liposomal components, including ETO. Notably, in the optimized formulations, the crystalline peak of ETO was absent (Fig. 3D, E). This finding is consistent with the observations of Mahdi Bahrami et al. (2023), who reported the absence of a doxorubicin peak, suggesting a transition from crystalline to amorphous state [50].

Analyses release of ETO from liposome

To evaluate the drug release profiles, in vitro release studies for free etodolac (ETO), formulation F1, and formulation F2 were conducted at pH 7.4 and 37°C, as well as at pH 5.4 and 39°C. The release profiles, expressed as cumulative percentage release over time, are presented in Fig. 3. At pH 7.4, free ETO exhibited a gradual release, reaching 31.3% ± *standard deviation* at 4 hours and 49.4% ± *standard deviation* at 24 hours (Fig. 3 A). In contrast, both liposomal formulations (F1 and F2) displayed a burst release at 4 hours, with 51.1% ± 0.05 and 72.3% ± 0.208 release, respectively. This was followed by a sustained release, reaching 89.9% ± 0.04 (F1) and 96.1% ± 0.055 (F2) at 24 hours (Fig. 3A). Similarly, at pH 5.4, a burst release was observed for F1 and F2 at 4 hours (53.1% ± 0.005 and 73.1% ± 0.036, respectively), followed by sustained release reaching 90.7% ± 0.045 (F1)

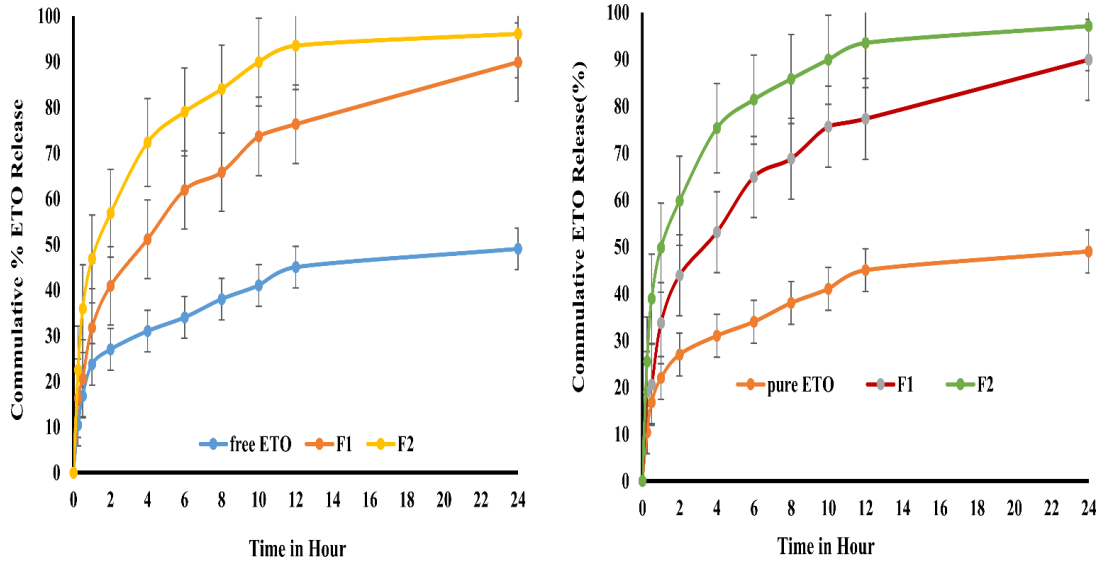

Fig. 3. Cumulative release profile of free ETO, conventional liposome (DSPC: CHOL), PEGylated lip liposome (DSPC: CHOL: DSPE-PEG2000), and target liposome (DSPC: CHOL: DSPE-PEG2000- DSPE-PEG2000-FA) at (A): pH 7.4 pH 7.4 and 37°C, and (B): pH 5.4 pH 7.4 and 39 °C.

and 97.1% ± 0.043 (F2) at 24 hours (Fig. 3B).

This biphasic release behavior of ETO from the liposomal formulations is characteristic of sustained-release systems, indicating an initial rapid release followed by a prolonged release phase. This sustained release is contingent upon the gradual diffusion of the drug from the liposomal membrane [51,52]. While the initial rapid release is likely attributed to the presence of drug loosely associated with the outer liposomal membrane or its high accessibility to the external environment, facilitating easy release. Furthermore, the release of ETO from liposomes under physiological conditions (pH 7.4) was lower than that observed under cancerous conditions (pH 5.4). This enhanced release at acidic pH may be attributed to liposomal swelling, disruption, and rupture, whereas the liposomes exhibited better drug retention under physiological pH.

Kinetic of release

As shown in Table 3, the Korsmeyer-Peppas model is the best-fit model for the optimal liposomal formulations at pH 7.4 and 5.4. Also shown in Table 3, the obtained (n) values in the Korsmeyer-Peppas kinetic model, which ranged from 0.243 to 0.34 for all samples, indicated the presence of an anomalous transport mechanism controlling the release of ETO from the prepared formulations. This suggests that the release of ETO from the liposome formulations occurs through a combination of diffusion through the lipid bilayers and erosion of the liposome matrix. These results are consistent with the findings of Anna Czajkowska et al. (2021), who mentioned that the release of ETO from nanostructured lipid carriers follows the Korsmeyer-Peppas model [53], and also consistent with the findings of Samet et al. (2023), who reported that the release of ETO from nanoemulsions follows the Korsmeyer-Peppas model [54,48].

Cytotoxicity

The cytotoxicity of blank and etodolac (ETO)-loaded liposomes on SW480 cells was evaluated using an MTT assay [29,30,31]. Blank liposomes (without ETO) showed minimal toxicity even at high concentrations (cell viability > 90%), indicating good biocompatibility, as shown in Fig. 4 A and B. Both etodolac (ETO) and ETO-loaded liposomes demonstrated concentration- and time-dependent cytotoxicity. Free ETO showed toxicity at higher concentrations (500–1000 µg/ml), while the liposomal formulations (F1, F2) were effective across the tested concentrations (128–1000 µg/ml), as listed in Table 4. The maximum cytotoxic effect for F1 and F2 was observed after 48 hours. ETO-loaded liposomes (F1 and F2) and pure ETO were tested at varying concentrations, revealing that F2, which contained (DSPC: CH: DSPE-PEG2000: DSPE-PEG2000-FA), exhibited significantly higher cytotoxicity (lower IC50) of 554.6 ± 9.12 and 128.88 ± 5.26 µg/ml at 24 and 48 hours, respectively. In contrast, F1, which contained (DSPC: CH), had IC50 values of 602.03 ± 2.8 and 419.33 ± 3.55 µg/ml at 24 and 48 hours. The IC50 for pure ETO was 713.72 ± 4.85 and 536.98 ± 6.23 µg/ml at 24 and 48 hours, respectively.

There were significant differences between the IC50 values of the different formulations and pure ETO ($p \leq 0.05$). The higher toxicity of the ETO-loaded liposome formulations compared to pure ETO is likely due to the high affinity of liposomes for the cell membrane. This result is

Table 3. Release kinetic models for Free ETO, F1, and F2 in buffer saline (pH 7.4) and in acetate buffer (pH 5.5).

Release kinetic models in buffer saline pH 7.4			
	Free ETO	F1	F2
Zero order	0.820	0.866	0.77
First order	0.8922	0.982	0.980
Higuchi	0.948	0.977	0.927
Korsmeyer-Peppas	0.989	0.995	0.983
n-exponent	0.275	0.34	0.216
Release kinetic models in Acetate buffer pH 5.5			
	Free ETO	F1	F2
Zero order	0.832	0.849	0.756
First order	0.897	0.979	0.979
Higuchi	0.955	0.969	0.918
Korsmeyer-Peppas	0.988	0.992	0.985
n-exponent	0.299	0.327	0.243

also consistent with the findings of Sang Min Lee et al. (2025), who reported that liposome-loaded DOX exhibited greater cytotoxicity than free DOX solution [40]. The enhanced cytotoxicity of F2 compared to F1 is likely due to the extended-release components of the ETO-loaded liposomes, leading to prolonged drug metabolism within cells and increased drug accumulation in tumor cells. This, combined with the specific targeting of folate receptors on SW480 cells, facilitated rapid internalization and prolonged drug action, resulting in a significantly enhanced antitumor effect. These results are consistent with Bing Han et al. (2020), who mentioned that targeted PTX liposomes showed higher cytotoxicity than non-targeted PTX liposomes due to a higher affinity toward estrogen receptors on MCF-7 cells [55].

The enhanced cytotoxicity of F2 compared to F1 is likely due to the extended-release components of the ETO-loaded liposomes, leading to prolonged drug metabolism within cells and increased drug accumulation in tumor cells. This, combined with the specific targeting of folate receptors on SW480 cells, facilitated rapid internalization and prolonged drug action, resulting in a significantly enhanced antitumor effect. These results are consistent with Bing Han et al. (2020), who reported higher cytotoxicity for targeted PTX liposomes compared to non-targeted PTX liposomes due to a higher affinity toward estrogen receptors on MCF-7 cells [56]. Improved cellular uptake is further supported by the negligible toxicity observed with the blank formulations, as shown in Fig. 4A and B.

Cellular uptake

To evaluate the efficacy of the optimized ETO liposome formulation in enhancing ETO uptake and internalization, SW480 human colorectal adenocarcinoma cells were selected as the target cell line. Due to ETO's poor aqueous solubility, a reference solution of pure ETO was prepared in a 1.4% v/v DMSO aqueous solution. As depicted in Fig. 4C, SW480 cell uptake was assessed after a 2-hour incubation with an equivalent amount of ETO (500 µg) delivered either as the pure ETO solution or within the optimized ETO liposome formulation. The cellular ETO uptake was measured at 12.54 ± 0.078 µg per 104 cells for the pure ETO in solution and 20.48 ± 0.19, and 26.31 ± 0.11 µg per 104 cells for the optimized F1 and F2 formulations, respectively. This demonstrates a statistically significant improvement in ETO uptake by SW480 cells when delivered via the optimized ETO formulation compared with the pure ETO reference solution (P=0.008197). Also, the result shows the targeted liposome F2 a higher cellular uptake compared with non-targeted liposome F1 loaded ETO (P=0.0051). Studies indicate that nanoparticles measuring 100 to 200 nm are optimal for tumor accumulation via the enhanced permeability and retention (EPR) effect, as they are large enough to avoid blood leakage but small enough to evade immune clearance [57].

The liposomes in this study, with a mean size of 125.5 nm, fall within this ideal range, supporting their potential for targeted cancer cell internalization. This aligns with previous research, such as Jin et al. (2016), which demonstrated effective cancer targeting with nanoparticles in the same size range [58]. In addition to that, the SW480 colon cancer cells have an overexpression of folate receptor [59], so folate-modified liposomes enable them to specifically target tumor cells by binding to folate receptors on the cell surface, which leads to enhanced cellular uptake and drug delivery of the targeted liposome. The receptor-ligand complex formation can trigger endocytic internalization, a mechanism with potential to augment nanoparticle cellular uptake and thereby enhance drug delivery efficacy [60]. This observation is corroborated by Yan Tie et al. (2020), who demonstrated the targeting of folate receptors of lung cancer cells by liposomes loaded with BIM-S plasmid modified with folate [61]. This observation is also corroborated by Suraj Baskararaj et al. (2020), who demonstrated that targeting of folate receptors (FRs) on a breast cancer cell model resulted in significantly increased liposome uptake via FR-mediated endocytosis, leading to heightened cytotoxicity [62]. These

Table 4. In Vitro Cytotoxicity (IC50 µg/ml) of Pure ETO, F1, and F2 at 24 and 48 Hours ± SD (n=3).

	IC50 µg/ml at 24hr.	IC50 µg/ml at 48hr.
Pure ETO	713.72± 4.85	536.98±6.23
F1	602.03±2.8	419.33±3.55
F2	554.6±9.12	128.88±5.26

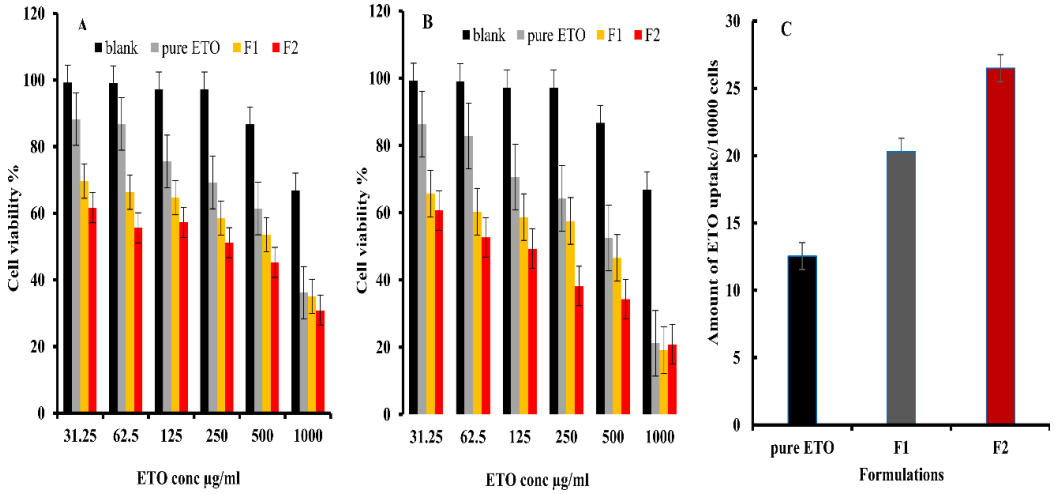

Fig. 4. SW480 cell survival after treatment with pure ETO and ETO-loaded liposomes using a concentration range of 31.25–1000 µg/ml for (A) 24 hours and (B) 48 hours. (C) In vitro cellular uptake of Etodolac from pure drug and optimized liposome formulations F1 and F2 in SW480 colon cancer cells.

Table 5. Stability Study of ETO-Loaded Liposomes F1 and F2 at 4°C and 25°C (n=3, ± SD).

Time day		F1			F2	
At 25°C	PZ nm	PDI	% EE	PZ nm	PDI	% EE
Initial	111.7±0.11	0.001	89.7%±0.002	125.5 ± 0.01	0.027	88.6%±0.017
15	119.9±0.01	0.04	87.6±0.02	129.3±0.007	0.001	88.1±0.1
30	125.4±0,06	0.08	85.9±0.3	130.7±0.06	0.003	87.8±0.25
45	130.6±0.14	0..04	83.9±0.93	131.7±0.03	0.02	85.1±0.05
60	131.5±0.022	0.07	83.8±1.3	133.8±0.07	0.025	84.7±0.16
			At 4°C			
Initial	111.7±0.11	0.001	89.7%±0.002	125.5 ± 1.99	0.027	88.6%±0.017
15	114.77±	0.008	88.7±0.05	126.8	0.056	87.8±0.17
30	119.76±	0.004	88.2±0.19	129.4	0.08	87.1±0.13
45	122.61±	0.07	87.8±1.2	130.3	0.06	85.5±1.7
60	123.22±	0.09	86.2±1.6	132.6	0.1	84.8±1.34

findings underscore the importance of receptor-mediated endocytosis as a key mechanism for targeted nanoparticle delivery.

Stability of liposome

Liposome stability, crucial for safe and effective use, is influenced by formulation and manufacturing. Monitoring particle size and polydispersity revealed that liposomes loaded with ETO maintained a consistent size over two months. The stability of the optimized ETO-loaded liposome formulations was assessed by storing them for 60 days at both room temperature (25°C) and 4°C, as detailed in Table 5. Particle size, polydispersity index (PDI), and %EE were measured every two weeks. The consistent particle size, low PDI, and good %EE values observed throughout the storage period demonstrate the excellent long-term stability of all liposome formulations. This result is consistent with the findings of Rais V et al. (2020), who reported the stability of cationic liposomes for two months [63], and also consistent with the findings of Matbou Riahi M et al. (2018), who reported the stability of celecoxib liposomes for 12 months at [64].

CONCLUSION

Folic acid-functionalized liposomes, optimized using a Plackett-Burman experimental design and composed of DSPC and cholesterol, were efficiently developed for the delivery of Etodolac using the thin-film hydration method. Key factors (DSPC and sonication variables (SV)) influencing liposome properties (particle size (PZ), polydispersity

index (PDI), lipid content (LC), and encapsulation efficiency (EE)) were identified. The optimal formulation, determined through optimization, consisted of 12.7 mg DSPC, 5 mg cholesterol, and 8 mg/ml Etodolac. This formulation yielded nanoliposomes with the following characteristics: for the optimum formula, (111.7 ± 0.11 nm, 0.001, 89.7% ± 0.002) for (PZ, PDI, and %EE) for formulation F1, and (125.5 ± 0.01 nm, 0.027, 88.6% ± 0.017) for formulation F2, respectively. The drug release was over 96.1% and 97.1% after 24 hours for F1 and F2, respectively. These experimental results closely matched the predictions from the Plackett-Burman experimental design. Differential scanning calorimetry (DSC) confirmed that Etodolac was dispersed within the nanoparticles in an amorphous or disordered-crystalline state. Fourier transform infrared spectroscopy (FT-IR) indicated no significant chemical interactions between Etodolac (ETO) and DSPC. Field scanning electron microscopy (FSEM) images showed that the ETO-loaded liposomes were well-dispersed, spherical, and exhibited a uniform size distribution. The optimized ETO-loaded liposomes demonstrated favorable properties, including small particle size, sustained drug release, long-term stability, and significantly enhanced cellular uptake in SW480 colon cancer cells compared to free Etodolac. These findings suggest a strong potential as a foundation for developing an effective colon-targeted drug delivery system.

CONFLICT OF INTEREST

The authors declare that there is no conflict of interests regarding the publication of this manuscript.

REFERENCE

1. Wilczewska AZ, Niemirowicz K, Markiewicz KH, Car H. Nanoparticles as drug delivery systems. Pharmacol Rep. 2012;64(5):1020-1037.
2. Abdel Hady M, Sayed OM, Akl MA. Brain uptake and accumulation of new levofloxacin-doxycycline combination through the use of solid lipid nanoparticles: Formulation; Optimization and in-vivo evaluation. Colloids Surf B Biointerfaces. 2020;193:111076.
3. Mudshinge SR, Deore AB, Patil S, Bhalgat CM. Nanoparticles: Emerging carriers for drug delivery. Saudi Pharmaceutical Journal. 2011;19(3):129-141.
4. El-Gamal FR, Akl MA, Mowafy HA, Mukai H, Kawakami S, Afouna MI. Synthesis and Evaluation of High Functionality and Quality Cell-penetrating Peptide Conjugated Lipid for Octaarginine Modified PEGylated Liposomes In U251 and U87 Glioma Cells. J Pharm Sci. 2022;111(6):1719-1727.
5. Akl MA, Eldeen MA, Kassem AM. Beyond Skin Deep: Phospholipid-Based Nanovesicles as Game-Changers in Transdermal Drug Delivery. AAPS PharmSciTech. 2024;25(6).
6. Antimisiaris SG, Kallinteri P, Fatouros DG. Liposomes and Drug Delivery. Pharmaceutical Manufacturing Handbook: Wiley; 2007. p. 443-533.
7. Khatun F, Toth I, Stephenson RJ. Immunology of carbohydrate-based vaccines. Adv Drug Del Rev. 2020;165-166:117-126.
8. Cummings RD. The mannose receptor ligands and the macrophage glycome. Curr Opin Struct Biol. 2022;75:102394.
9. Riaz M, Riaz M, Zhang X, Lin C, Wong K, Chen X, et al. Surface Functionalization and Targeting Strategies of Liposomes in Solid Tumor Therapy: A Review. Int J Mol Sci. 2018;19(1):195.
10. Wicki A, Witzigmann D, Balasubramanian V, Huwyler J. Nanomedicine in cancer therapy: Challenges, opportunities, and clinical applications. Journal of Controlled Release. 2015;200:138-157.
11. Noble GT, Stefanick JF, Ashley JD, Kiziltepe T, Bilgicer B. Ligand-targeted liposome design: challenges and fundamental considerations. Trends Biotechnol. 2014;32(1):32-45.
12. Sawant RR, Torchilin VP. Challenges in Development of Targeted Liposomal Therapeutics. The AAPS Journal. 2012;14(2):303-315.
13. Keum N, Giovannucci EL. Epidemiology of Colorectal Cancer. Pathology and Epidemiology of Cancer: Springer International Publishing; 2016. p. 391-407.
14. Siegel RL, Miller KD, Jemal A. Cancer statistics, 2019. CA Cancer J Clin. 2019;69(1):7-34.
15. Maniewska J, Jeżewska D. Non-Steroidal Anti-Inflammatory Drugs in Colorectal Cancer Chemoprevention. Cancers (Basel). 2021;13(4):594.
16. Tremi I, Nowsheen S, Aziz K, Siva S, Ventura J, Hatzi VI, et al. Inflammation and oxidatively induced DNA damage: A synergy leading to cancer development. Cancer: Elsevier; 2021. p. 131-147.
17. Newman P, Muscat J. Potential Role of Non-Steroidal Anti-Inflammatory Drugs in Colorectal Cancer Chemoprevention for Inflammatory Bowel Disease: An Umbrella Review. Cancers (Basel). 2023;15(4):1102.
18. Okamoto A, Shirakawa T, Bito T, Shigemura K, Hamada K, Gotoh A, et al. Etodolac, a Selective Cyclooxygenase-2 Inhibitor, Induces Upregulation of E-Cadherin and Has Antitumor Effect on Human Bladder Cancer Cells In Vitro and In Vivo. Urology. 2008;71(1):156-160.
19. Balfour JA, Buckley MMT. Etodolac. Drugs. 1991;42(2):274-299.
20. Talari R, Varshosaz J, Mostafavi SA, Nokhodchi A. Gliclazide Microcrystals Prepared by Two Methods of In Situ Micronization: Pharmacokinetic Studies in Diabetic and Normal Rats. AAPS PharmSciTech. 2010;11(2):786-792.
21. Rainsford KD. Ibuprofen: pharmacology, efficacy and safety. Inflammopharmacology. 2009;17(6):275-342.
22. El-Sonbaty MM, Akl MA, El-Say KM, Kassem AA. Does the technical methodology influence the quality attributes and the potential of skin permeation of Luliconazole loaded transethosomes? J Drug Deliv Sci Technol. 2022;68:103096.
23. Akl MA, Ryad S, Ibrahim MF, Kassem AA. Formulation, and optimization of transdermal Atorvastatin Calcium-Loaded Ultra-flexible vesicles; ameliorates poloxamer 407-caused dyslipidemia. Int J Pharm. 2023;638:122917.

24. Mahdy MAA, Akl MA, Madkour FA. Effect of chitosan and curcumin nanoparticles against skeletal muscle fibrosis at early regenerative stage of glycerol-injured rat muscles. BMC Musculoskeletal Disorders. 2022;23(1).
25. Barakat EH, Akl MA, Ibrahim MF, Mohamed Dawaba H, Afouna MI. Formulation and optimization of theophylline-loaded enteric-coated spanlastic nanovesicles for colon delivery; Ameliorate acetic acid-induced ulcerative colitis. Int J Pharm. 2023;643:123253.
26. Jaiswal S, Gupta GD. Optimization, Formulation, and Ex vivo Evaluation of Solid Lipid Nanoparticles for Transdermal Delivery of Diltiazem Hydrochloride. Pharmaceutical Nanotechnology. 2024;13.
27. Akl MA, Ismael HR, Abd Allah FI, Kassem AA, Samy AM. Tolmetin sodium-loaded thermosensitive mucoadhesive liquid suppositories for rectal delivery; strategy to overcome oral delivery drawbacks. Drug Development and Industrial Pharmacy. 2018;45(2):252-264.
28. El-Sonbaty MM, Ismail HR, Kassem AA, Samy AM, Akl MA. Mucoadhesive thermoreversible formulation of metoclopramide for rectal administration: a promising strategy for potential management of chemotherapy-induced nausea and vomiting. Pharmaceutical Development and Technology. 2020;25(5):535-546.
29. Real-Time Label-Free Targeting Assessment and in Vitro Characterization of Curcumin-Loaded Poly-lactic-co-glycolic Acid Nanoparticles for Oral Colon Targeting. American Chemical Society (ACS). http://dx.doi.org/10.1021/acsomega.9b02086.s001
30. Akl MA, Kartal-Hodzic A, Oksanen T, Ismael HR, Afouna MM, Yliperttula M, et al. Factorial design formulation optimization and in vitro characterization of curcumin-loaded PLGA nanoparticles for colon delivery. J Drug Deliv Sci Technol. 2016;32:10-20.
31. Yamamoto H, Kuno Y, Sugimoto S, Takeuchi H, Kawashima Y. Surface-modified PLGA nanosphere with chitosan improved pulmonary delivery of calcitonin by mucoadhesion and opening of the intercellular tight junctions. Journal of Controlled Release. 2005;102(2):373-381.
32. Pattadar DK, Zamborini FP. Effect of Size, Coverage, and Dispersity on the Potential-Controlled Ostwald Ripening of Metal Nanoparticles. Langmuir. 2019;35(50):16416-16426.
33. Sahu AK, Jain V. Screening of process variables using Plackett–Burman design in the fabrication of gedunin-loaded liposomes. Artificial Cells, Nanomedicine, and Biotechnology. 2016;45(5):1011-1022.
34. Hassan M, Essam T, Yassin AS, Salama A. Optimization of rhamnolipid production by biodegrading bacterial isolates using Plackett–Burman design. Int J Biol Macromol. 2016;82:573-579.
35. Pawar HA, Attarde VB, Parag Subhash G. Optimization of Bifonazole-Loaded Nisomal Formulation Using Plackett-Burman Design and 2 Factorial Design. Open Pharmaceutical Sciences Journal. 2016;3(1):31-48.
36. Sallam L, El-Refai AM, El-Kady I. ChemInform Abstract: umwandlung von progesteron durch aspergillus niger 100 und rhizopus nigricans ref, 129. Chemischer Informationsdienst Organische Chemie. 1970;1(32).
37. Handali S, Moghimipour E, Rezaei M, Ramezani Z, Kouchak M, Amini M, et al. A novel 5-Fluorouracil targeted delivery to colon cancer using folic acid conjugated liposomes. Biomedicine & Pharmacotherapy. 2018;108:1259-1273.
38. Mohanty D, Rani MJ, Haque MA, Bakshi V, Jahangir MA, Imam SS, et al. Preparation and evaluation of transdermal naproxen niosomes: formulation optimization to preclinical anti-inflammatory assessment on murine model. J Liposome Res. 2019;30(4):377-387.
39. Shilakari Asthana G, Asthana A, Singh D, Sharma PK. Etodolac Containing Topical Niosomal Gel: Formulation Development and Evaluation. Journal of Drug Delivery. 2016;2016:1-8.
40. Sharma N, Madan P, Lin S. Effect of process and formulation variables on the preparation of parenteral paclitaxel-loaded biodegradable polymeric nanoparticles: A co-surfactant study. Asian Journal of Pharmaceutical Sciences. 2016;11(3):404-416.
41. Akl MA, Ryad S, Ibrahime MF, Kassem AA. Ultraflexible liposomes for transdermal delivery of atorvastatin calcium: Rheological and ex vivo evaluation. Eur J Lipid Sci Technol. 2024;126(11).
42. Amul B, Muthu S, Raja M, Sevvanthi S. Spectral, DFT and molecular docking investigations on Etodolac. J Mol Struct. 2019;1195:747-761.
43. Mustafa WW, Khoder M, Abdelkader H, Singer R, Alany RG. Interactions of Cyclodextrins and their Hydroxyl Derivatives with Etodolac: Solubility and Dissolution Enhancement. Curr Drug Del. 2024;21(1):126-139.
44. Patil M, Pandit P, Udavant P, Sonawane S, Bhambere D. Development and Optimization of Proniosomal Gel Containing Etodolac: In-vitro, Ex-vivo and In-vivo Evaluation. Ars Pharmaceutica (Internet). 2021;62(3):290-304.
45. Sherje AP, Kulkarni V, Murahari M, Nayak UY, Bhat P, Suvarna V, et al. Inclusion Complexation of Etodolac with Hydroxypropyl-beta-cyclodextrin and Auxiliary Agents: Formulation Characterization and Molecular Modeling Studies. Mol Pharm. 2017;14(4):1231-1242.
46. Bilge D, Sahin I, Kazanci N, Severcan F. Interactions of tamoxifen with distearoyl phosphatidylcholine multilamellar vesicles: FTIR and DSC studies. Spectrochimica Acta Part A: Molecular and Biomolecular Spectroscopy. 2014;130:250-256.
47. Sharma G, Mahajan A, Thakur K, Kaur G, Goni VG, Kumar MV, et al. Exploring the therapeutic potential of sodium deoxycholate tailored deformable-emulsomes of etodolac for effective management of arthritis. Sci Rep. 2023;13(1).
48. Salah S, Mahmoud AA, Kamel AO. Etodolac transdermal cubosomes for the treatment of rheumatoid arthritis: ex vivo permeation and in vivo pharmacokinetic studies. Drug Deliv. 2017;24(1):846-856.
49. Alesskndrany A, Sahin I. The effects of Levothyroxine on the structure and dynamics of DPPC liposome: FTIR and DSC studies. Biochim Biophys Acta. 2020;1862(6):183245.
50. Bahrami Parsa M, Tafvizi F, Chaleshi V, Ebadi M. Preparation, characterization, and Co-delivery of cisplatin and doxorubicin-loaded liposomes to enhance anticancer Activities. Heliyon. 2023;9(10):e20657.
51. Gill V, Nanda A. Preparation And Characterization of Etodolac Bearing Emulsomes. International Journal of Applied Pharmaceutics. 2020:166-172.
52. Pal A, Gupta S, Jaiswal A, Dube A, Vyas SP. RETRACTED ARTICLE Development and evaluation of tripalmitin emulsomes for the treatment of experimental visceral leishmaniasis. J Liposome Res. 2011;22(1):62-71.
53. Czajkowska-Kośnik A, Szymańska E, Czarnomysy R, Jacyna J, Markuszewski M, Basa A, et al. Nanostructured Lipid Carriers

Engineered as Topical Delivery of Etodolac: Optimization and Cytotoxicity Studies. Materials. 2021;14(3):596.
54. Özdemir S, Üner B, Karaküçük A, Çelik B, Sümer E, Taş Ç. Nanoemulsions as a Promising Carrier for Topical Delivery of Etodolac: Formulation Development and Characterization. Pharmaceutics. 2023;15(10):2510.
55. Lee SM, Yoo S-Y, Kim T, Kim N, Kang J, Lim K-Y, et al. Radiopaque hydrogel-in-liposomes towards theranostic applications for malignant tumors. Biomedicine & Pharmacotherapy. 2025;183:117822.
56. Han B, Yang Y, Chen J, Tang H, Sun Y, Zhang Z, et al. Preparation, Characterization, and Pharmacokinetic Study of a Novel Long-Acting Targeted Paclitaxel Liposome with Antitumor Activity. International Journal of Nanomedicine. 2020;Volume 15:553-571.
57. Shigehiro T, Kasai T, Murakami M, Sekhar SC, Tominaga Y, Okada M, et al. Efficient Drug Delivery of Paclitaxel Glycoside: A Novel Solubility Gradient Encapsulation into Liposomes Coupled with Immunoliposomes Preparation. PLoS One. 2014;9(9):e107976.
58. Jin H, Pi J, Yang F, Jiang J, Wang X, Bai H, et al. Folate-Chitosan Nanoparticles Loaded with Ursolic Acid Confer Anti-Breast Cancer Activities in vitro and in vivo. Sci Rep. 2016;6(1).
59. Sultana N, David AE. Improving Cancer Targeting: A Study on the Effect of Dual-Ligand Density on Targeting of Cells Having Differential Expression of Target Biomarkers. Int J Mol Sci. 2023;24(17):13048.
60. Joseph JG, Liu AP. Mechanical Regulation of Endocytosis: New Insights and Recent Advances. Advanced Biosystems. 2020;4(5).
61. Tie Y, Zheng H, He Z, Yang J, Shao B, Liu L, et al. Targeting folate receptor β positive tumor-associated macrophages in lung cancer with a folate-modified liposomal complex. Signal Transduction and Targeted Therapy. 2020;5(1).
62. Baskararaj S, Panneerselvam T, Govindaraj S, Arunachalam S, Parasuraman P, Pandian SRK, et al. Formulation and characterization of folate receptor-targeted PEGylated liposome encapsulating bioactive compounds from Kappaphycus alvarezii for cancer therapy. 3 Biotech. 2020;10(3).
63. Pavlov RV, Gaynanova GA, Kuznetsova DA, Vasileva LA, Zueva IV, Sapunova AS, et al. Biomedical potentialities of cationic geminis as modulating agents of liposome in drug delivery across biological barriers and cellular uptake. Int J Pharm. 2020;587:119640.
64. Matbou Riahi M, Sahebkar A, Sadri K, Nikoofal-Sahlabadi S, Jaafari MR. Stable and sustained release liposomal formulations of celecoxib: In vitro and in vivo anti-tumor evaluation. Int J Pharm. 2018;540(1-2):89-97.